

10<sup>th</sup> International Conference on Applied Energy (ICAE2018), 22-25 August 2018, Hong Kong, China

# Weighted pseudo-inverse based control allocation of heterogeneous redundant operating mechanisms for distributed propulsion configuration

Zhihui Wang<sup>a</sup>, Jing Zhang<sup>a</sup>, Lingyu Yang<sup>a,\*</sup>

<sup>a</sup>*School of Automation Science and Electrical Engineering, Beihang University, Beijing 100191, China*

---

## Abstract

Distributed propulsion configuration (DPC) usually have heterogeneous redundant operating mechanisms including redundant control surfaces and thrust vector actuators, thus producing strong and complex control coupling between flight and propulsion systems. Then control allocation of heterogeneous redundant actuators is certainly required to realize integrated control. First, the formulation of this specific control allocation problem is given, and then the Moore-Penrose pseudo-inverse method and weighted pseudo-inverse method are introduced to improve control accuracy and coordinate the complex relationship between different types of actuators. Simulation results reveal that the weighted pseudo-inverse method has higher accuracy in allocation result, and it is suitable for the specific control allocation problem for DPC aircraft.

© 2019 The Authors. Published by Elsevier Ltd.

This is an open access article under the CC BY-NC-ND license (<http://creativecommons.org/licenses/by-nc-nd/4.0/>)

Peer-review under responsibility of the scientific committee of ICAE2018 – The 10th International Conference on Applied Energy.

**Keywords:** distributed propulsion configuration, heterogeneous redundant actuators, control allocation, weighted pseudo-inverse method

## 1. Introduction

The adverse impact of the aviation activities on the environment is mainly reflected in noise, air quality, energy consumption, and greenhouse gas emissions. To reduce this impact, next-generation civil aircraft development plans are proposed in Europe and the United States, such as SAX-40 and N3-X [1-6].

---

\* Corresponding author. Tel.: +86-312-82316873; fax: +86-312-83217332.

E-mail address: [yanglingyu@buaa.edu.cn](mailto:yanglingyu@buaa.edu.cn)

The new aircraft design concept of distributed propulsion configuration (DPC) is adopted by the next-generation civil aircrafts. DPC's primary features include: 1) the blended wing body (BWB) layout can significantly improve the lift/drag characteristics [7]; 2) the use of several sets of semi-buried propulsion system can take the initiative to achieve active adjustment of aerodynamic and load distribution. Meanwhile, thrust vector technology and new types of multiple control surfaces, such as ailerons and winglet rudders, are also applied in next-generation civil aircrafts. Redundant control surfaces and thrust vector actuators form heterogeneous multiple operating mechanisms, which produce an increased coupling effect between engines and the aircraft. Thus, control allocation is strongly demanded.

The pseudo-inverse method was first used to reconstruct the redundant system when control surfaces failed [8]. The control efficiency matrix directly reflects the performance relationship between the control surface deflection angles and the aerodynamic torque that can be generated [9] [10]. Due to the different speed limits of the aircraft's different control surfaces, the bandwidth is different. Therefore, different control surfaces should be designed with different weights [11]. The weighted pseudo-inverse method improves the pseudo-inverse method under this idea.

In this paper, a specific DPC aircraft is selected as the object. First, the characteristics of DPC aircraft and the formulation of control allocation to be solved are described. Then, pseudo-inverse method is analyzed with the optimal target of lowest energy consumption. To improve the reliability, coordinate the relationship between various surfaces and ensure the lowest energy consumption at the same time, weighted pseudo-inverse method is proposed. Finally, these two methods are simulated and analyzed.

## Nomenclature

$\mathbf{v}$	virtual control input, $m \times 1$
$\mathbf{u}$	true control input, $n \times 1$
$\mathbf{B}$	control effectiveness matrix, $m \times n$
$\mathbf{P}, \mathbf{P}_w$	a generalized inverse of a matrix $\mathbf{B}$ , $n \times m$
$\mathbf{u}_{\min}, \mathbf{u}_{\max}$	lower/upper limits of $\mathbf{u}$ , $n \times 1$
$\lambda$	an n-vector of LaGrange multipliers, $n \times 1$
$\mathbf{W}_u$	weighting matrix, $n \times n$
$\Phi$	attainable moment subset, AMS, $\Phi \subset \mathbf{R}^m$
$\mathbf{err}$	control allocation error, $m \times 1$
ratio	ratio of generalized inverse method AMS to system AMS
pinv	the Moore-Penrose pseudo-inverse method
wpinv	the weighted pseudo-inverse method
$diag(\text{vector})$	a square matrix whose diagonal elements are elements of $\text{vector}$ , $n \times n$
$L, M, N$	roll/pitch/yaw moment (J)
$T$	thrust (N)
$\delta_{l1}, \delta_{r2}$	left/right inside elevon deflection angle (degree)
$\delta_{l2}, \delta_{r2}$	left/right middle elevon deflection angle (degree)
$\delta_{l3}, \delta_{r3}$	left/right outside elevon deflection angle (degree)
$\delta_{w1}, \delta_{w2}$	left/right winglet rudder deflection angle (degree)
$\pi_{kl}^*, \pi_{lm}^*, \pi_{kr}^*$	the pressure ratio of the left/middle/right turbo fan
$A_{sl}, A_{sm}, A_{sr}$	the turbo nozzle outlet area of left/middle/right engine ( $\text{m}^2$ )
$\alpha_{ll}, \alpha_{lm}, \alpha_{lr}$	thrust vectoring angle of left/middle/right engine in vertical direction (degree)
$\beta_{ll}, \beta_{lm}, \beta_{lr}$	thrust vectoring angle of left/middle/right engine in horizontal direction (degree)

## 2. Description of DPC aircraft and control allocation

This study addresses the control allocation of the DPC aircraft to produce required roll, pitch, yaw moments and thrust.

## 2.1. Description of DPC aircraft

As shown in Fig. 1. The DPC aircraft has six elevons and two winglet rudders at the edge of wings and also three engines with nine fans at the end of fuselage. It has no horizontal tails. These features produce strong coupling effect in roll and yaw channels, which makes control more difficult. These three engines adopt Two-Dimensional (2-D) thrust vector technology, and each engine has a variable exhaust nozzle at the duct exits. Meanwhile, fan pressure ratio of engines is variable.

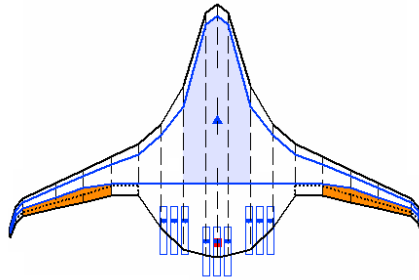


Fig. 1. Control surfaces configuration of DPC aircraft [2]

## 2.2. Formulation of control allocation

The control allocation problem is that of distributing a desired total control effort among a redundant set of actuators [9]. It is formulated as follows. Given  $\mathbf{B}, \mathbf{v}, \mathbf{u}_{\min}$  and  $\mathbf{u}_{\max}$ , find  $\mathbf{u}$  such that,

$$\mathbf{B}\mathbf{u} = \mathbf{v}, \quad \mathbf{u}_{\min} \leq \mathbf{u} \leq \mathbf{u}_{\max} \quad (1)$$

where

$$\begin{aligned} \mathbf{v} &= [L, M, N, thrust]^T, \\ \mathbf{u} &= [\delta_{l1}, \delta_{r2}, \delta_{l2}, \delta_{r2}, \delta_{l3}, \delta_{r3}, \delta_{w1}, \delta_{w2}, \pi_{kl}^*, A_{8l}, \pi_{km}^*, A_{8m}, \pi_{kr}^*, A_{8r}, \alpha_{tl}, \beta_{tl}, \alpha_{tm}, \beta_{tm}, \alpha_{tr}, \beta_{tr}]^T, \\ &\begin{cases} -60^\circ \leq \delta_{l1}, \delta_{r2}, \delta_{l2}, \delta_{r2}, \delta_{l3}, \delta_{r3}, \delta_{w1}, \delta_{w2} \leq 60^\circ \\ 1 \leq \pi_{kl}^*, \pi_{km}^*, \pi_{kr}^* \leq 1.6 \\ 1 \leq A_{8l}, A_{8m}, A_{8r} \leq 1.6 \\ -30^\circ \leq \alpha_{tl}, \beta_{tl}, \alpha_{tm}, \beta_{tm}, \alpha_{tr}, \beta_{tr} \leq 30^\circ \end{cases} \end{aligned} \quad (2)$$

Equation (1) can be considered as a linear mapping under the control effectiveness matrix  $\mathbf{B}$

$$\mathbf{B}: \mathbf{R}^n \rightarrow \mathbf{R}^m \quad (3)$$

However,  $\mathbf{B}$  may change according to the vector  $\mathbf{u}$ , but it is fixed during every simulation step.

The space of equation (1) is marked as subset  $\Omega$ ,

$$\Omega = \{\mathbf{u} \in \mathbf{R}^n | \mathbf{u}_{\min} \leq \mathbf{u} \leq \mathbf{u}_{\max}\} \subset \mathbf{R}^n \quad (4)$$

Under the linear mapping (3),  $\Phi$  is defined as follows,

$$\mathbf{B}: \Omega \rightarrow \Phi \quad (5)$$

where  $\Phi \subset \mathbf{R}^m$  is called attainable moment subset (AMS): a subset of all moments [12].

The set of equation (1) is under-determined (fewer equations than unknowns) and mathematically has an infinite number of solutions. When control limitations are introduced the equations may have no solutions [13].

## 3. Control allocation based on generalized inverse

How to find the best solution of equation (1) is a realistic problem, especially when there are infinitely many solutions. In this section, pseudo-inverse method is introduced and proved. All the control variables participate in the control during the entire flight. Therefore, the total deflection of the aerodynamic control surfaces can be reduced. However,  $\mathbf{u}$  contains different kinds of control inputs. It is unreasonable to treat them equally. For this

reason, weighted pseudo-inverse method is adopted. Its indicator is to minimize the 2-norm of the vector  $\mathbf{W}_u \mathbf{u}$ . Obviously, additional fuel is required. But it is flexible when we want to adjust the deflection of actuators during different flight phases and under different mission requirements by changing weighting matrix  $\mathbf{W}_u$ .

### 3.1. The Moore-Penrose pseudo-inverse method

A particular generalized inverse of a matrix  $\mathbf{B}$  is  $\mathbf{P}$  that will minimize the 2-norm of our control vector  $\mathbf{u}$  when solving the control allocation problem. The 2-norm of a vector is just its length, the positive square-root of the sum of the squares of the individual controls. This generalized inverse is known as the Moore–Penrose pseudo-inverse.

When matrix  $\mathbf{B}$  is full rank and the limits  $\mathbf{u}_{\min}, \mathbf{u}_{\max}$  are ignored, the formula (1) has an infinite number of solutions. We can find the only one using the Moore–Penrose pseudo-inverse method.

And the true control input is

$$\mathbf{u} = \mathbf{B}^T (\mathbf{B}\mathbf{B}^T)^{-1} \mathbf{v} = \mathbf{P}\mathbf{v} \quad (6)$$

where  $\mathbf{P} = \mathbf{B}^T (\mathbf{B}\mathbf{B}^T)^{-1}$ .

It is proved as follows.

Using LaGrange multipliers, we define the scalar function

$$H(\mathbf{u}, \lambda) = \frac{1}{2} \mathbf{u}^T \mathbf{u} + \lambda^T (\mathbf{v} - \mathbf{B}\mathbf{u}) \quad (7)$$

The factor of 1/2 anticipates that there will be a 2 to cancel.  $H$  will be a minimum (or maximum) when

$$\frac{\partial H}{\partial \mathbf{u}} = \mathbf{0}, \quad \frac{\partial H}{\partial \lambda} = \mathbf{0} \quad (8)$$

Performing the operations yields

$$\frac{\partial H}{\partial \mathbf{u}} = \mathbf{u}^T - \lambda^T \mathbf{B} = \mathbf{0} \quad (9)$$

Hence, we require that  $\mathbf{u}^T = \lambda^T \mathbf{B}$ , or  $\mathbf{u} = \mathbf{B}^T \lambda$ .

$$\frac{\partial H}{\partial \lambda} = \mathbf{v} - \mathbf{B}\mathbf{u} = \mathbf{0} \quad (10)$$

So that,  $\mathbf{v} = \mathbf{B}\mathbf{u}$ . Now combining the two results

$$\mathbf{v} = \mathbf{B}\mathbf{u} = \mathbf{B}\mathbf{B}^T \lambda \quad (11)$$

Since  $\mathbf{B}$  is full rank,  $\mathbf{B}^T \mathbf{B}$  is too, and since  $\mathbf{B}^T \mathbf{B}$  is square it is invertible. Thus

$$\lambda = (\mathbf{B}\mathbf{B}^T)^{-1} \mathbf{v} \quad (12)$$

Since  $\mathbf{u} = \mathbf{B}^T \lambda$  we have

$$\mathbf{u} = \mathbf{B}^T (\mathbf{B}\mathbf{B}^T)^{-1} \mathbf{v} = \mathbf{P}\mathbf{v} \quad (13)$$

where  $\mathbf{P} = \mathbf{B}^T (\mathbf{B}\mathbf{B}^T)^{-1}$ .  $\square$

The principal claim made about the minimum-norm pseudo-inverse is that because it minimizes the sum of the squares of the control effector displacements, it thus minimizes the consumption of energy of all actuators.

### 3.2. Weighted pseudo-inverse method

The Moore–Penrose is just one of an infinity of closed-form inverses that minimizes a vector norm. Entire families of these solutions can be obtained from optimization problems that aim to minimize other norms of  $\mathbf{u}$ . The weighted 2-norm is seen frequently. And it is to minimize  $\mathbf{u}^T \mathbf{W}_u^T \mathbf{W}_u \mathbf{u}$ , where  $\mathbf{W}_u$  is a positive diagonal matrix.

The solution of equation (1) using weighted pseudo-inverse method is given:

$$\mathbf{u} = \mathbf{W}_u^{-1} \mathbf{B}^T (\mathbf{B}\mathbf{W}_u^{-1} \mathbf{B}^T)^{-1} \mathbf{v} = \mathbf{P}_w \mathbf{v} \quad (14)$$

where  $\mathbf{P}_w = \mathbf{W}_u^{-1} \mathbf{B}^T (\mathbf{B}\mathbf{W}_u^{-1} \mathbf{B}^T)^{-1}$ .

It is easy to get equation (14) replacing  $\mathbf{u}$  of  $\mathbf{W}_u \mathbf{u}$  from equation (7) ~ (13).  $\square$

Regarding the issue above, the Moore-Penrose pseudo-inverse method and weighted pseudo-inverse method can be used to solve control allocation problem under their optimal index.

#### 4. Simulation

In this section, a special DPC aircraft is chosen with parameters and flight state point data shown in Table 1.

Table 1. geometric parameters and flight data of a special DPC aircraft

Parameter	Value
Wing area, m <sup>2</sup>	836
Wing span, m <sup>2</sup>	63.22
C.G., % centerbody chord	58.3
Maximum take-off weight, Kg	150,847
Flight height, m	5,000
Mach	0.6
Angle of attack for trim, degree	1.72

Now consider a specially chosen virtual control input  $\mathbf{v} = [-10435529, 6147752, -707065, 265852]^T$ . And

$$\mathbf{B}_{pinv\_aero} = \begin{bmatrix} 9.89E5 & -9.89E5 & 1.11E6 & -1.11E6 & 1.22E6 & -1.22E6 & -7.03E3 & -7.03E3 \\ -5.63E5 & -5.63E5 & -3.63E5 & -3.63E5 & -1.62E5 & -1.62E5 & 8.78E3 & 8.78E3 \\ 3.77E3 & -3.77E3 & 2.39E4 & -2.39E4 & 2.39E4 & -2.39E4 & -1.03E5 & -1.03E5 \\ 0 & 0 & 0 & 0 & 0 & 0 & 0 & 0 \end{bmatrix},$$

$$\mathbf{B}_{pinv\_eng} = \begin{bmatrix} 0 & 0 & 0 & 0 & 0 & 0 \\ 0 & 0 & 0 & 0 & 0 & 0 \\ 0 & 0 & 0 & 0 & 0 & 0 \\ 235700 & 46180 & 235700 & 46180 & 23570 & 46180 \end{bmatrix}, \mathbf{B}_{pinv\_vt} = \begin{bmatrix} -1.08E4 & 0 & 0 & 0 & 1.08E4 & 0 \\ 2.70E4 & 0 & 2.70E4 & 0 & 2.70E4 & 0 \\ 0 & 2.70E4 & 0 & 2.70E4 & 0 & 2.70E4 \\ 0 & 0 & 0 & 0 & 0 & 0 \end{bmatrix}.$$

If we ignore the small difference between  $\mathbf{B}_{pinv}$  and  $\mathbf{B}_{wpinv}$ , then they are approximately equal.

In order to make full use of the elevons and winglet rudders and make the difference between  $\pi_k^*$  and  $A_k$ , we choose  $\mathbf{W}_u = \text{diag}([1/60, 1/60, 1/60, 1/60, 1/60, 1/60, 1/60, 1/10, 1/21, 1/10, 1/21, 1/10, 1/21, 1/25, 1/25, 1/25, 1/25, 1/25])$ .

Table 2. Results of control allocation using two methods.

Parameters	pinv	wpinv
True control input	$\mathbf{u}_{pinv}$	$\mathbf{u}_{wpinv}$
2-norm of $\mathbf{u}$	8.81	8.94
2-norm of $\mathbf{W}_u \mathbf{u}$	--	0.32
AMS	See Fig. 3	See Fig. 4
ratio	53.23 %	50.46 %
$\mathbf{err}$	$\mathbf{err}_{pinv}$	$\mathbf{err}_{wpinv}$
$\ \mathbf{err}\ _2$	1.6632	1.4560
maximum error	1.4580	1.4248
number of iterations	20	20
average running time, s	0.99	0.95

We can easily calculate the solution of the system, according to equation (13) and (14), see Table 2.

$$\mathbf{u}_{pinv} = [-4.74, -2.49, -4.02, -0.63, -2.86, 0.77, 2.35, 2.35, 1.43, 1.33, 1.43, 1.33, 1.43, 1.33, 0.18, -0.60, 0.17, -0.60, 0.16, -0.60]^T$$

$$\mathbf{u}_{wpinv} = [-3.94, -3.30, -4.43, -0.23, -3.14, 1.06, 2.29, 2.29, 1.42, 1.40, 1.42, 1.40, 1.42, 1.40, 0.03, -0.41, 0.03, -0.41, 0.03, -0.41]^T,$$

$$\mathbf{err}_{pinv} = [-0.0146, 0.7883, -0.1371, -1.4580]^T, \mathbf{err}_{wpinv} = [1.0625E-5, 0.0640, -0.2930, -1.4248]^T.$$

It is found that left inside elevon deflection angle  $\delta_{l1}$ , right middle elevon deflection angle  $\delta_{r2}$  and thrust vectoring angles  $\alpha_{l1}, \alpha_{lm}, \alpha_{lr}, \beta_{l1}, \beta_{lm}, \beta_{lr}$  are reduced fully. Roll and pitch moments are compensated by the increase of the rest of elevons' angle. Aerodynamic surfaces are used more effectively than before. This is consistent with the principle of using as little thrust vector as possible due to its limited service life.

From **B**, we can see that thrust and moment are completely decoupled. So, we delete the forth row of **B** and use the rest to obtain AMS, see Fig. 3 and Fig. 4. The volume formed by the red line donates AMS using generalized inverse method, while blue section donating system AMS. Ratio becomes smaller from 53.23% to 50.46%.

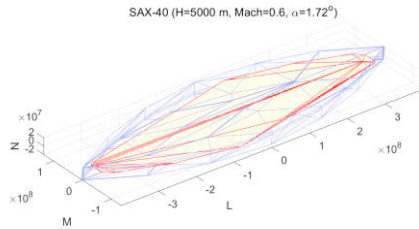


Fig. 3. AMS with the Moore-Penrose pseudo-inverse method

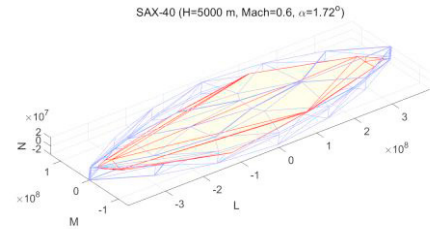


Fig. 4. AMS with the weighted pseudo-inverse method

## Conclusions

The new design concept of DPC and heterogeneous multiple operating mechanisms redundancy expand control space, and they also strengthen the coupling effect between flight and propulsion system. To solve the problem caused by strong coupling and operating mechanisms redundancy, control allocation is needed. This paper utilizes the weighted pseudo-inverse method to achieve control allocation with the minimum fuel energy consumption. However, weighting matrix is fixed during the entire simulation. Next work is to automatically adjust  $\mathbf{W}_u$  online.

## Acknowledgements

The authors would like to thank Wenwen Kang and YiQiang Xu for providing preliminary knowledge and data of DPC aircraft used in this paper. This work was supported by the National Natural Science Foundation of China (Grant No.61304030).

## References

- [1] Hileman, James. "Development of approach procedures for silent aircraft." 45th AIAA Aerospace Sciences Meeting and Exhibit. 2007.
- [2] De la Rosa Blanco, Elena, et al. "Challenges in the silent aircraft engine design." 45th AIAA Aerospace Sciences Meeting and Exhibit. 2007.
- [3] Tam, Ryan. "Assessment of Silent Aircraft-Enabled Regional Development and Airline Economics in the UK." 45th AIAA Aerospace Sciences Meeting and Exhibit. 2007.
- [4] J. I. Hileman, Z. S. Spakovszky, M. Drela. "Airframe Design for Silent Aircraft." 45th AIAA Aerospace Sciences Meeting and Exhibit, 2007
- [5] Thomas, Steve, and Ann Dowling. "A dynamical model and controller for the silent aircraft: the effect of maneuvering on noise." 45th AIAA Aerospace Sciences Meeting and Exhibit. 2007.
- [6] Martin M. D'Angelo GE Aviation, Lynn, Massachusetts John Gallman Vicki Johnson. "N+3 Small Commercial Efficient and Quiet Transportation for Year 2030-2035." [R] NASA/CR, 216691, 2010, 5-10.
- [7] Ziqiang, Zhu, et al. "A new type of transport-blended wing body aircraft." Acta Aeronautica et Astronautica Sinica-Series A and B- 29.1 (2008): 49.
- [8] Härkegård, Ola, and S. Torkel Glad. "Resolving actuator redundancy—optimal control vs. control allocation." Automatica 41.1 (2005): 137-144.
- [9] Bordignon, Kenneth A, et al. "Constrained Control Allocation for Systems with Redundant Control Effectors." Virginia Tech (1996).
- [10] Eberhardt, Rowena, and D. Ward. "Indirect adaptive flight control of a tailless fighter aircraft." Guidance, Navigation, and Control Conference and Exhibit 1999.
- [11] Durham, Wayne C. "Constrained control allocation." Journal of Guidance, Control, and Dynamics 16.4 (1993): 717-725.
- [12] Durham, W. "Attainable moments for the constrained control allocation problem." Journal of Guidance Control & Dynamics 17.6(1994):1371-1373.
- [13] Durham, Wayne C. "Computationally Efficient Control Allocation." Journal of Guidance Control & Dynamics 24.24(2001):519-524.